3-Hydroxy-1H-quinazoline-2,4-dione derivatives as new antagonists at ionotropic glutamate receptors: Molecular modeling and pharmacological studies

ARTICLE *in* EUROPEAN JOURNAL OF MEDICINAL CHEMISTRY · JUNE 2012

Impact Factor: 3.45 · DOI: 10.1016/j.ejmech.2012.05.036 · Source: PubMed

15 AUTHORS, INCLUDING:

Vittoria Colotta
University of Florence
113 PUBLICATIONS **1,643** CITATIONS
SEE PROFILE

Daniela Catarzi
University of Florence
101 PUBLICATIONS **1,473** CITATIONS
SEE PROFILE

Flavia Varano
University of Florence
81 PUBLICATIONS **1,268** CITATIONS
SEE PROFILE

Lucia Squarcialupi
University of Florence
12 PUBLICATIONS **62** CITATIONS
SEE PROFILE

European Journal of Medicinal Chemistry 54 (2012) 470–482

Contents lists available at SciVerse ScienceDirect

European Journal of Medicinal Chemistry

journal homepage: http://www.elsevier.com/locate/ejmech

Original article

3-Hydroxy-1*H*-quinazoline-2,4-dione derivatives as new antagonists at ionotropic glutamate receptors: Molecular modeling and pharmacological studies

Vittoria Colotta [a,*], Ombretta Lenzi [a], Daniela Catarzi [a], Flavia Varano [a], Lucia Squarcialupi [a], Chiara Costagli [b], Alessandro Galli [b], Carla Ghelardini [b], Anna Maria Pugliese [b], Giovanna Maraula [b], Elisabetta Coppi [b], Domenico E. Pellegrini-Giampietro [b], Felicita Pedata [b], Davide Sabbadin [c], Stefano Moro [c]

[a] *Dipartimento di Scienze Farmaceutiche, Laboratorio di Progettazione, Sintesi e Studio di Eterocicli Biologicamente Attivi, Universita' di Firenze, Polo Scientifico, Via Ugo Schiff 6, 50019 Sesto Fiorentino, FI, Italy*

[b] *Dipartimento di Farmacologia Preclinica e Clinica, Università degli Studi di Firenze, Viale Pieraccini 6, 50139 Firenze, Italy*

[c] *Molecular Modeling Section (MMS), Dipartimento di Scienze del Farmaco, Università degli Studi di Padova, via Marzolo 5, 35131 Padova, Italy*

HIGHLIGHTS

- Heterocyclic rings at the 6-position gave good AMPA receptor affinity.
- Derivative **8** (R_6 = 1,2,4-triazol-4-yl) showed high AMPA receptor affinity.
- Derivative **3** showed the best affinity and selectivity for the kainate receptor.
- Derivatives **3** and **8** were effective neuroprotective agents in rat models of cerebral ischemia.
- Compound **8** showed anticonvulsant effect in pentylenetetrazole-induced convulsions.

GRAPHICAL ABSTRACT

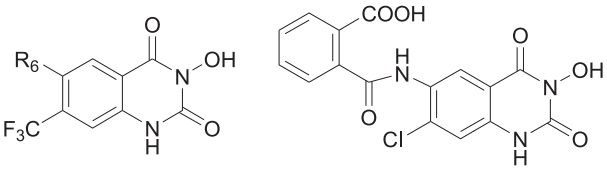

R_6= H, NO_2, NH_2, Heterocycle, 2-COOH-C_6H_4-CONH

ARTICLE INFO

Article history:
Received 20 December 2011
Received in revised form
21 May 2012
Accepted 23 May 2012
Available online 4 June 2012

Keywords:
Ionotropic glutamate receptors
3-Hydroxyquinazoline-2,4-diones
AMPA receptor antagonists
Kainate receptor antagonists
Neuroprotective agents
Ligand–receptor modeling studies

ABSTRACT

Based on our 3-hydroxy-7-chloroquinazoline-2,4-dione derivatives, previously reported as antagonists at ionotropic glutamate receptors, we synthesized new 3-hydroxyquinazoline-2,4-diones bearing a trifluoromethyl group at the 7-position and different groups at position 6. Glycine/NMDA, AMPA and kainate receptor binding data showed that the 7-trifluoromethyl residue increased AMPA and kainate receptor affinity and selectivity, with respect to the 7-chlorine atom. Among the probed 6-substituents, the 6-(1,2,4-triazol-4-yl) group (compound **8**) was the most advantageous for AMPA receptor affinity and selectivity. Derivative **8** demonstrated to be effective in decreasing neuronal damage produced by oxygen and glucose deprivation in organotypic rat hippocampal slices and also showed anticonvulsant effects in pentylenetetrazole-induced convulsions. The previously reported kainate receptor antagonist 6-(2-carboxybenzoyl)-amino-7-chloro-3-hydroxyquinazoline-2,4-dione **3** prevented the failure of neurotransmission induced by oxygen and glucose deprivation in the CA1 region of rat hippocampal slices.

Abbreviations: Glu, glutamate; iGluRs, ionotropic glutamate receptors; NMDA, *N*-methyl-D-aspartate; AMPA, (*S*)-2-amino-3-(3-hydroxy-5-methyl-4-isoxazolyl)propionic acid; KA, kainate; DCKA, 5,7-dichlorokynurenic acid; NBQX, 2,3-dihydroxy-6-nitro-7-sulphamoyl-benzo[*f*]quinoxaline; MK-801, (+)-5-methyl-10,11-dihydro-5*H*-benzo[*a*,*d*]cyclohepten-5,10-iminemaleate; PTZ, pentylenetetrazole; OGD, oxygen and glucose deprivation; PI, propidium iodide; fepsp, field excitatory postsynaptic potential; AD, anoxic depolarization; aCSF, artificial cerebrospinal fluid.

* Corresponding author. Tel.: +39 055 4573731; fax: +39 055 4573780.
E-mail address: vittoria.colotta@unifi.it (V. Colotta).

0223-5234/$ – see front matter
http://dx.doi.org/10.1016/j.ejmech.2012.05.036

1. Introduction

Glutamate (Glu) is the major excitatory neurotransmitter in the mammalian central nervous system and plays key roles in regulating many physiological processes through activation of metabotropic (mGluRs) and ionotropic receptors (iGluRs) [1,2]. The iGluRs include three families classified as *N*-methyl-D-aspartate (NMDA), (*S*)-2-amino-3-(3-hydroxy-5-methyl-4-isoxazolyl) propionic acid (AMPA) and kainate (KA) receptors. The NMDA receptor complex possesses different binding sites including the glutamate co-agonist glycine binding site (Gly/NMDA) [2]. To date, seven NMDA receptor subunits (GluN1, GluN2A-2D, and GluN3A and GluN3B), four AMPA receptor subunits (GluA1-GluA4) and five KA receptor subunits (GluK1-GluK5) have been cloned and characterized [2]. It is well known that an overstimulation of iGluRs induce an increase of intracellular Ca^{2+} concentrations, release of K^+ into the extracellular space and cell swelling due to the passive movement of water with Na^+ influx [3]. The massive increase of intracellular Ca^{2+} triggers numerous deleterious processes, including free radical formation and membrane degradation, mitochondrial dysfunction, inflammation, DNA-damage and apoptosis. These processes lead to neuronal death and are implicated in many diseases [1] such as Alzheimer's [4] and Parkinson's diseases [5], amyotrophic lateral sclerosis [6], epilepsy [1,7] and cerebral ischemia [8].

Due to the iGluR-mediated excitotoxicity, several compounds acting as iGluR antagonists demonstrated beneficial effects against the above cited pathologies [1,4,5].

It has to be noted that AMPA and KA receptor antagonists seem to possess greater therapeutic potential than NMDA antagonists because these latter often show adverse effects such as hallucinations, agitation, ataxia and catatonia [9].

In the last decade, a part of our research has been focused on the study of competitive and noncompetitive iGluR antagonists, belonging to different heteroaromatic systems [10–21]. Among them, the 3-hydroxyquinazoline-2,4-dione was disclosed as a useful scaffold to obtain selective iGluR antagonists [15,18], since many derivatives of this series showed affinity for AMPA and KA receptors or for the Gly/NMDA site. The 3-hydroxyquinazolin-2,4-diones possess the most important structural requirements for Gly/NMDA and AMPA or KA receptor recognition [22,23]: a flat hydrophobic area represented by the fused benzo ring; a NH hydrogen-bond donor that binds a proton acceptor of the receptor; a δ-negatively charged moiety, represented by both the 2-carbonyl group and the 3-hydroxy substituent, able to form a hydrogen bond with a cationic hydrogen bond donor receptor site. All the previously described 3-hydroxyquinazoline-2,4-dione derivatives (Fig. 1) are substituted at the 7-position with a chlorine atom that is combined with different substituents at the 6-position. Structure–affinity relationship (SAR) studies suggested that the nature of the 6-substituents was critical for the selectivity towards the different iGluRs. In particular, $R_6 = H$ gave a selective Gly/NMDA antagonist (compound **1**), while heterocyclic rings gave AMPA receptor antagonists, the most advantageous was the 6-(1,2,4-triazol-4-yl) moiety (derivative **2**) [15]. Instead, the presence of a 6-(2-carboxybenzoyl)-amino group on the 3-hydroxyquinazoline-2,4-dione scaffold afforded a selective KA receptor antagonist (compound **3**) [18]. On the basis of these results, we decided to continue the study of this class of compounds to further investigate the SARs and to obtain more potent AMPA and/or KA receptor antagonists. Thus, we planned the synthesis of new 6-substituted 3-hydroxyquinazoline-2,4-dione derivatives (Fig. 2, compounds **4**–**11**) in which the 7-chlorine atom was replaced with a 7-trifluoromethyl residue that was thought to increase affinity towards AMPA and KA receptors [12,16]. The 6-position of the new derivatives bears the substituents

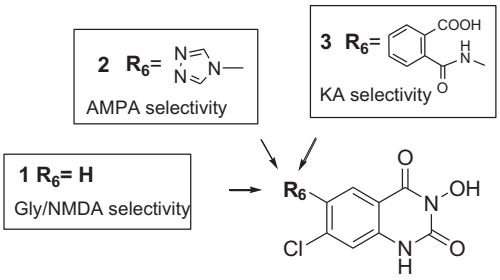

Fig. 1. Previously reported 7-chloro-3-hydroxyquinazoline-2,4-dione derivatives.

which in previous studies turned out to be profitable for the AMPA or KA receptor affinity and selectivity, i.e. heterocyclic rings or the 2-carboxybenzoylammino group, respectively.

2. Chemistry

The target compounds **4**–**11** were synthesized as described in Schemes 1 and 2. The 7-trifluoromethyl-1,2-dihydro-3,1-benzoxazine-2,4-dione **12** [21] was reacted with O-benzylhydroxylamine in refluxing ethanol to give the 2-amino-*N*-benzyloxy-4-trifluoromethylbenzamide **13**. Cyclization of **13** with triphosgene afforded the 3-benzyloxy-7-trifluoromethylquinazoline-2,4-dione **14** which was debenzylated with 48% HBr in glacial acetic acid to give the desired 3-hydroxy derivative **4**. This latter was transformed into the corresponding 3-acetate **15** by refluxing in acetic anhydride. Nitration of **15** with 90% HNO_3 afforded the corresponding 6-nitro compound **16** that was transformed into the 6-amino derivative **17**. Reaction of **17** with phthalic anhydride afforded the desired 3-hydroxy-6-(2-carboxybenzoylamino)-quinazoline-2,4-dione **7**. The 3-hydroxy-6-nitroquinazoline-2,4-dione **5**, its corresponding 6-amino derivative **6** and the 6-heteroaryl substituted compounds **8**–**11** were synthesized as shown in Scheme 2. Derivative **12** was reacted with O-methylhydroxylamine to yield the 2-amino-3-methoxy-4-trifluoromethylbenzamide **18** which was cyclized with triphosgene to give derivative **19**. Nitration of **19** afforded 6-nitro-3-methoxy derivative **20** which was desmethylated with 48% hydrobromic acid in glacial acetic acid to give the 3-hydroxy-6-nitroquinazoline-2,4-dione **5**. Catalytic reduction (Pd/C) of compound **5** gave the 6-amino derivative **6**.

To prepare the 7-trifluoromethyl-3-hydroxy-6-(1,2,4-triazol-4-yl)-quinazoline-2,4-dione **8**, compound **20** was reduced to the corresponding 6-amino compound **21** that was transformed into **22** by reaction with diformylhydrazine. Different attempts to turn the 3-O-methyl derivative **22** into the corresponding 3-hydroxy derivative **8** failed. In fact, treatment of **22** with boron tribromide at room temperature for three to four days left compound **22** unmodified, while reaction with 48% aqueous hydrobromic acid in glacial acetic acid at 100 °C afforded the 6-amino compound **6**. Thus, the desired derivative **8** was obtained by reacting compound **6** with

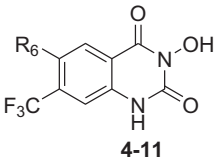

4-11

R_6= H, NO_2, NH_2, Heterocycle, 2-COOH-C_6H_4-CONH

Fig. 2. Currently reported 3-hydroxyquinazoline-2,4-dione derivatives.

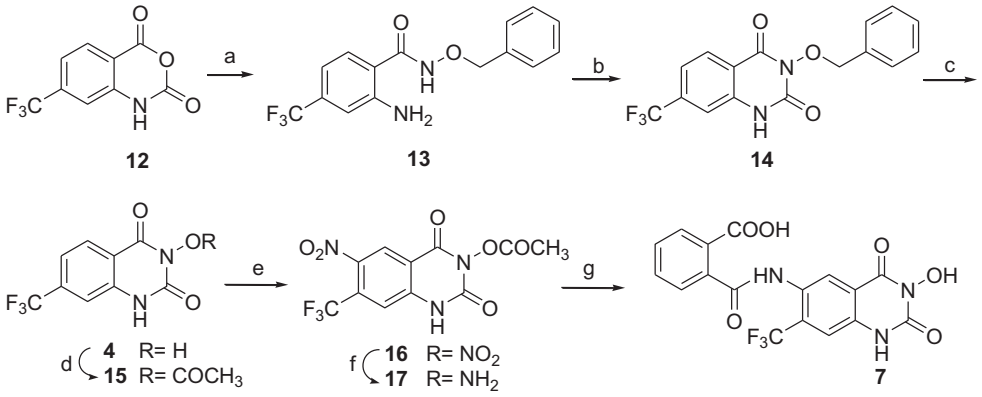

Scheme 1. Reagents and conditions. (a) O-Benzylhydroxylamine hydrochloride, NEt_3, EtOH, reflux; (b) triphosgene, NEt_3, r.t.; c) 48% HBr, glacial AcOH, reflux; d) Ac_2O, reflux; e) 90% HNO_3, from −10 to 0 °C; f) H_2, Pd/C, EtOH; g) (i) phthalic anhydride, NaOAc, 60 °C; (ii) 0.25 M NaOH, r.t.; (iii) 6 N HCl.

diformylhydrazine. Reaction of **6** with 2,5-diethoxytetrahydrofuran or 2,5-dimethoxytetrahydrofuran-3-carbaldehyde in glacial acetic acid at 90 °C gave, respectively, the 6-(pyrrol-1-yl)- derivative **9** and the 6-(3-formylpyrrol-1-yl)- substituted compound **10**. This latter was oxidized with potassium permanganate in water/acetone to give the 6-(3-carboxypyrrol-1-yl)- derivative **11**.

3. Results and discussion

3.1. Structure–affinity relationship

The newly synthesized 7-trifluoromethyl-3-hydroxyquinazoline-2,4-dione derivatives **4**–**11** and the synthetic intermediate **22**, 3-*O*-methyl analog of the 6-(1,2,4-triazolyl)-substituted derivative **8**, were evaluated for their binding at AMPA, Gly/NMDA and high-affinity KA receptors in rat cortical membranes. The binding data are shown in Table 1, together with those of the previously reported 7-chloroquinazolines **1**–**3**, **23**–**25** [15,18], included as reference compounds. Table 1 also displays the affinities of 5,7-dichlorokyunurenic acid (DCKA) and of 2,3-dihydroxy-6-nitro-7-sulphamoyl-benzo[*f*]quinoxaline (NBQX), well-known antagonists of the Gly/NMDA and AMPA receptors, respectively. The obtained results were coherent with our expectations. Replacement of the 7-chlorine atom with the 7-trifluoromethyl group positively affected the binding at the AMPA receptor. In fact, derivatives **4**, **5**, **8**, **10** and **11** possess an increased AMPA affinity with respect to those of the corresponding 7-cloro derivatives **1**, **23**, **2**, **24** and **25** [15,18]. Compound **4**, lacking the 6-substituent, has a good affinity for the

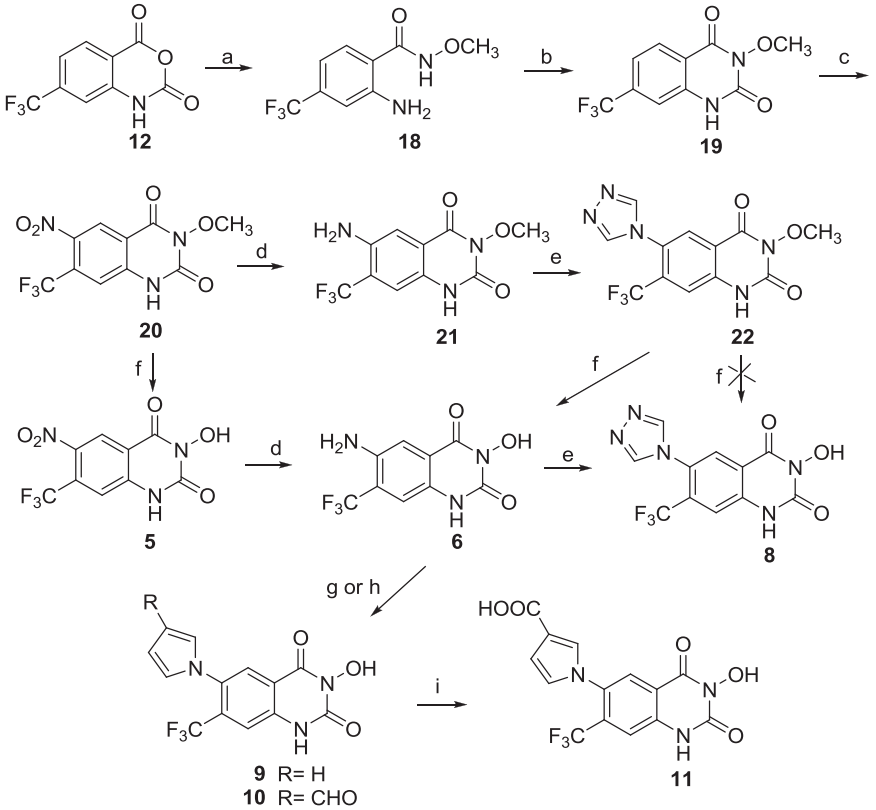

Scheme 2. Reagents and conditions. (a) O-Methylhydroxylamine hydrochloride, NEt_3, EtOH, reflux; (b) triphosgene, NEt_3, r.t.; c) 90% HNO_3, from −10 to 0 °C; d) H_2, Pd/C, EtOH; e) diformylhydrazine, Me_3SiCl, anhydrous pyridine, 100 °C; f) 48% HBr, glacial AcOH, reflux; g) 2,5-diethoxytetrahydrofuran, glacial AcOH; h) 2,5-diethoxytetrahydrofuran-3-carbaldehyde, glacial AcOH; (i) $KMnO_4$, H_2O/acetone (1:1), 0 °C; (ii) 38% sodium hydrogen sulfite; (iii) 6 N HCl.

Table 1
Binding affinity at AMPA, Gly/NMDA and high-affinity KA receptors.

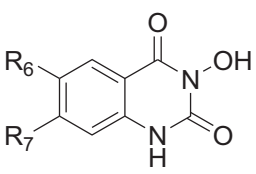

1-11, 23-25

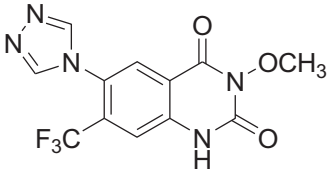

22

compd	R_6	R_7	K_i (μM)[a] or I%[b]		IC_{50} (μM)[c] or I%[b]	log BB_{pred}[e]
			[^{3}H]AMPA	[^{3}H]glycine	[^{3}H]KA	
1[d]	H	Cl	11.6 ± 1.9	0.24 ± 0.02	140 ± 15	−0.08
2[d]		Cl	0.25 ± 0.04	47%	7.0 ± 0.5	−0.74
3[d]	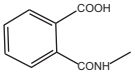	Cl	16.5 ± 1.2	40%	0.62 ± 0.02	−0.86
23[d]	NO_2	Cl	1.3 ± 0.1	1.1 ± 0.1	19.1 ± 1	−0.11
24[d]		Cl	4.2 ± 0.1	22.7 ± 2.7	6.2 ± 0.4	−0.45
25[d]	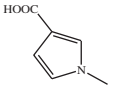	Cl	1.3 ± 0.2	44%	13 ± 0.6	−1.19
4	H	CF_3	4.8 ± 0.4	0.85 ± 0.09	37.6 ± 7.0	−0.03
5	NO_2	CF_3	0.26 ± 0.02	1.3 ± 0.06	7.0 ± 0.5	−0.02
6	NH_2	CF_3	6.1 ± 6.2	6.1 ± 6.5	32 ± 4	−0.07
7	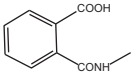	CF_3	8%	10%	25 ± 4	−0.74
8		CF_3	0.08 ± 0.007	6.5 ± 0.8	3.0 ± 0.3	−0.57
9		CF_3	126 ± 9	32%	10%	−0.20
10		CF_3	0.72 ± 0.13	0.8 ± 0.1	4.2 ± 0.3	−0.31
11	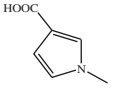	CF_3	0.46 ± 0.04	5.1 ± 0.9	17.3 ± 3	−0.98
22			20 ± 2.5	21%	0%	−0.38
DCKA			5%	0.08 ± 0.02	8%	−0.10
NBQX			0.07 ± 0.06	3%	7.0 ± 1.1	−0.11

[a] K_i values are means ± SEM of three or four separate determinations in triplicate.
[b] Percentage of inhibition (I%) of specific binding at 100 μM concentration.
[c] IC_{50} values were means ± SEM of three or four separate determinations in triplicate.
[d] References [15,18].
[e] Predicted blood–brain barrier permeation (log BB_{pred} = log [Brain]/[Blood]).

Gly/NMDA receptor (K_i = 0.85 μM), while it binds the AMPA and KA receptors with lower affinities (K_i = 4.8 μM and 37.6 μM, respectively). Introduction of substituents at the 6-position of compound **4** differently affected receptor affinity and selectivity. The presence of the 6-NO_2 group (derivative **5**) shifted affinity toward the AMPA receptor (K_i = 0.26 μM), while the 6-NH_2 substituent afforded a nonselective Gly/NMDA *versus* AMPA receptor antagonist (derivative **6**). The 6-heterocycle-substituted compounds **8**, **10** and **11** possess good to high AMPA receptor affinities and different degrees of selectivity, the most interesting being the 6-(1,2,4-triazolo-1-yl)-substituted derivative **8** which displayed the highest AMPA receptor affinity (K_i = 0.08 μM) and selectivity *versus* both Gly/NMDA and KA receptors. These results confirm that the 1,2,4-triazol-4-yl moiety is one of the most profitable heterocyclic rings to obtain potent and selective AMPA receptor antagonists. Good AMPA receptor affinity was also shown by the 6-(3-formyl-1*H*-pyrrol-1-yl)- substituted derivative **10** (K_i = 0.72 μM) and the 6-(3-carboxypyrrol-1-yl)-substituted compound **11** (K_i = 0.46 μM), even though they are less

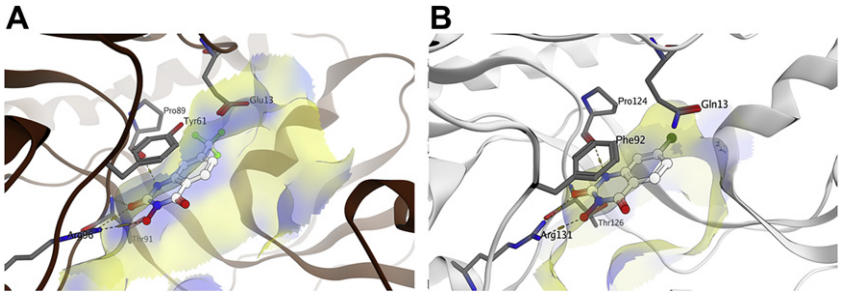

Fig. 3. Comparison between AMPA and Gly/NMDA receptor surface properties at the top of the binding pocket with one of the new quinazoline-2,4-dione derivatives. Molecular surface of receptors in contact with ligands has been highlighted. Hydrophobic area is colored in yellow and polar areas of the binding pocket are depicted in blue. The peculiar hydrogen bonding network involving Arg 96, Thr 91 and Pro 89 of the AMPA receptor (Panel A), and the homologous Arg 131, Thr 126, and Pro 124 of the Gly/NMDA receptor (Panel B), with the reported compounds (compound **4**, panel A and compound **1**, panel B) is shown in orange. An additional π–π stacking interaction between Tyr 61 side chain at the AMPA (Phe 92 at the Gly/NMDA) receptor and the 3-hydroxyquinazoline-2,4-dione scaffold is also common to all related derivatives. (For interpretation of the references to colour in this figure legend, the reader is referred to the web version of this article.)

AMPA selective than compound **8**. It is interesting to note that both the 3-formyl and the 3-carboxy group on the 6-pyrrole ring play a key role for the binding at all three receptors since their removal significantly reduced the affinity (compare compounds **10** and **11** with the 6-pyrrol-1-yl-substituted compound **9**). Introduction of the 2-carboxybenzoylamino group at position 6 of the parent compound **4** annulled both AMPA and Gly/NMDA receptor affinity and maintained the ability to bind the KA receptor (derivative **7**). Actually, compound **7** was expected to possess a higher KA receptor affinity, with respect to the corresponding 7-chloro derivative **3**. In fact, replacement of the chlorine atom with the trifluoromethyl group ameliorated not only the affinity for the AMPA receptor but also for the KA receptor (compare new compounds **4**, **5**, **8**, **10**, **11** to the corresponding 7-chloro derivatives **1**, **23**, **2**, **24** and **25**). The 3-O-methylation of compound **4** caused a drastic reduction of the binding affinity at the three receptors (compound **22**), thus confirming the importance of the free 3-hydroxy group in this class of derivatives.

3.2. Molecular modeling studies

Molecular modeling studies were carried out to rationalize the observed SARs, thus suggesting the hypothetical binding mode of these new antagonists at the Gly/NMDA and AMPA receptors.

The synthesized compounds were docked, using a genetic algorithm, into the putative binding sites of each receptor single subunit which structure has been determined by X-ray crystallography (See Section 5.2 for further details). Analysis of docking results highlighted a peculiar ligand–receptor interaction motif represented by a hydrogen bonding network involving the highly conserved residue triad among iGluRs: Arg 96, Thr 91 and Pro 89 at the AMPA receptor (Fig. 3A), and the homologous Arg 131, Thr 126, and Pro 124 at the Gly/NMDA receptor (Fig. 3B). An additional π–π stacking interaction, between the aromatic amino acid side chain located at the top of the binding pocket (Tyr 61 at the AMPA, and the homologous Phe 92 at the Gly/NMDA receptor), with the quinazoline-2,4-dione scaffold suggested that the binding motif of these newly synthesized antagonists could be compatible with the poses shown in Fig. 4A. This hypothesis is also confirmed by the recently published quinazolinedione sulfonamide derivative bound to human GluR2 [24].

Docking results at the AMPA receptor site showed that the NH group of compound **8** acts as a proton donor toward the backbone C=O of Pro 89, while the 2-carbonyl group accepts a hydrogen bond from the backbone NH of Thr 91 (Fig. 4A). Moreover, both 2-carbonyl and 3-hydroxy groups of compound **8** interact with the side chain of Arg 96. The triazole ring at the R_6-position accepts a hydrogen bond from the Thr 174 side chain. This specific polar interaction can explain the difference between the AMPA receptor affinities of compounds **8** and **9**. In fact, compound **9** completely lacks interaction with Thr 174, as shown in Fig. 4A. Interestingly, the 1,2,4-triazole ring of derivative **8** is directed toward Thr 174 in the AMPA receptor, which is mutated to Ala 206 in the Gly/NMDA receptor (Fig. 4B). This mutation is located in one of the less conserved regions between iGluRs and has the direct consequence of weakening the ligand–receptor interactions network, thus justifying the selectivity profile of the 6-(1,2,4-triazole) substituted derivative **8** (Table 1).

In the Gly/NMDA receptor site, the NH group of compounds **1** (Fig. 3B) and **4** acts as a proton donor toward the backbone C=O of Pro 124, while the 2-carbonyl group accepts a hydrogen bond from the backbone NH of Thr 126. Both the 2-carbonyl and 3-hydroxy

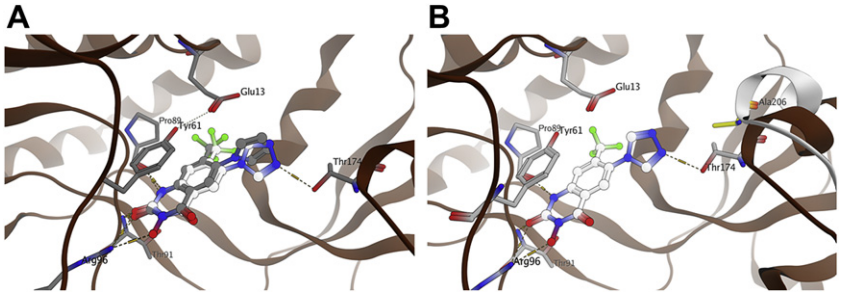

Fig. 4. *Panel A*: Predicted binding mode of compounds **8** (in white) and **9** (in gray) into the binding pocket of the AMPA receptor. *Panel B*: The R_6 substituent is directed towards the less conserved region between iGluRs, where Thr 174 (AMPA) - Ala 206 (Gly/NMDA – depicted in yellow) mutation is present. AMPA receptor ribbon, colored in brown, is shown. A part of Gly/NMDA receptor ribbon representation, where Ala 206 is located, is colored in white and is shown in figure. Receptor–ligand hydrogen-bonding interactions are depicted in orange. (For interpretation of the references to colour in this figure legend, the reader is referred to the web version of this article.)

groups of compounds **1** and **4** were found to interact with the Arg 131 side chain. Compound **4** ($R_7 = CF_3$) exhibited an increased binding affinity to AMPA receptors compared to compound **1** ($R_7 = Cl$) and, intriguingly, this trend was reversed on the Gly/NMDA receptor (Table 1). The peculiar effect observed around position 7 of the quinazoline scaffold can be associated to the important changes of the receptor surface properties in this specific region of the receptor cavities. In fact, the highly polar residues located at the top of the AMPA receptor binding pocket, such as Glu 13 and Tyr 61, are replaced with the more hydrophobic residues Gln 13 and Phe 92, in the Gly/NMDA receptor (Fig. 3). Following our modeling results, the change of the selectivity profiles of compounds **1** and **4** can be explained by the modification of the electrostatic potential surface properties of the two receptor areas around position 7 of the quinazoline scaffold.

Finally, blood brain barrier (BBB) penetration, plasma protein binding (PPB) and human intestinal absorption (HIA) were computed using StarDrop [25]. The predicted BBB penetration data (Table 1) were promising for several compounds (drugs with a poor ability to cross BBB typically have a log BB value ≤ -1.0), and in particular for the most interesting compounds of the series, i.e. **4** and **8**, showing the highest affinity and selectivity for the Gly/NMDA and AMPA receptor, respectively. Finally, the PPB and HIA predictions were encouraging for all the novel antagonists (unpublished data) based on the binary prediction models implemented by StarDrop software (HIA threshold = 30% absorbed; PPB threshold = 80% absorbed) [25].

3.3. Pharmacological studies

3.3.1. Functional antagonism studies

The antagonistic effect of some selected derivatives was evaluated both at the NMDA and AMPA receptors. Functional antagonism at the NMDA receptor-ion channel complex of compounds **4** and **8** was evaluated by measuring their ability to inhibit the stimulated binding of the NMDA receptor channel blocking agent [^{3}H](+) MK-801 [19]. The results are reported in Table 2, together with that of DCKA included as reference antagonist at the glycine site. Derivatives **4** and **8** demonstrated an antagonistic behavior with potencies correlated with their Gly/NMDA affinities.

Derivatives **8**, **10** and **11**, together with NBQX and DCKA as reference compounds, were assayed for their ability to inhibit depolarization induced by 5 μM AMPA and NMDA in cortical wedge preparations [14]. The results, reported in Table 2, showed that compounds **8**, **10** and **11** inhibited AMPA and NMDA responses with potencies which match their binding affinities. In fact, compounds **8** and **11** were the most active in inhibiting, respectively, AMPA- and NMDA-evoked responses, coherently with their AMPA and Gly/NMDA receptor affinities. It has to be noted that compound **8** potency is similar to that of NBQX in counteracting AMPA-induced depolarization.

Table 2
Inhibition of stimulated [^{3}H] (+)MK-801 binding and functional antagonism at NMDA and AMPA sites.

compd	[^{3}H] (+)MK-801 binding[a]	AMPA and NMDA induced depolarization[d]	
	IC_{50} (μM)[b]	IC_{50} (μM)[b]	
		NMDA	AMPA
4	7.2 ± 0.9	Nt[c]	Nt[c]
8	14 ± 0.9	24 ± 3	0.17 ± 0.02
10	Nt[c]	7.0 ± 1.0	1.5 ± 0.2
11	Nt[c]	>50	2.9 ± 0.35
DCKA	0.74 ± 0.09	4.7 ± 0.9	52 ± 11
NBQX	Nt[c]	(*)[e]	0.20 ± 0.02

[a] Inhibition of stimulated [^{3}H] (+)MK-801 binding. All assays were carried out in the presence of 10 μM glutamate and 0.1 μM glycine.
[b] IC_{50} values are means ± SEM of three or four separate determinations in triplicate.
[c] Not tested.
[d] Inhibition of depolarization induced by S-AMPA or NMDA in mouse cortical wedge preparation.
[e] At 10 μM concentration the inhibition was not significant.

Table 3
Anticonvulsant effect against PTZ-induced convulsions.

Treatment	Dose mg/kg p.o.	n. of mice	% Protection on PTZ-induced convulsions[a]
Vehicle	–	41	0
Compound **8**	30	24	65.5
Diazepam	1.0	30	93.3

[a] Pentylenetetrazole (PTZ) 90 mg/kg i.p.

3.3.2. Anticonvulsant studies

In our previous studies some 7-chloro-3-hydroxyquinazoline-2,4-diones showed anticonvulsant properties [20], therefore we decided to test compound **8** to evaluate its protective effect from convulsions in mice using pentylentetrazole (PTZ) as a chemical convulsant agent. Compound **8**, administered per os, exerted a significant anticonvulsant effect at 30 mg/kg (Table 3), thus showing both a good oral absorption and a good ability to penetrate the BBB, in line with the predicted BBB permeation (Table 1).

3.3.3. Oxygen–glucose deprivation (OGD) in organotypic rat hippocampal slice cultures

Compound **8**, which showed the highest AMPA receptor affinity and selectivity among the herein reported compounds, was tested in an *in vitro* model of cerebral ischemia to assess its efficacy in decreasing neuronal damage produced by oxygen and glucose deprivation (OGD) in organotypic rat hippocampal slices. It has been previously reported that OGD-neurotoxicity is significantly attenuated by adding either NMDA or AMPA receptor antagonists in the incubation medium during the 30 min insult and the subsequent 24 h recovery period [26,27]. Neuronal cell death was quantified using cellular uptake of the fluorescent dye propidium iodide (PI). When rat hippocampal slices incubated with PI were exposed to glutamate, fluorescence levels increased dramatically in virtually all neuronal populations. Maximal damage was achieved in this system by exposing the slices to 10 mM glutamate for 24 h. Exposure to OGD for 30 min caused a fluorescence pattern in which PI staining was more intense in the CA1 area of hippocampus [26]. In our experiments, quantitative analysis, carried out in the hippocampal CA1 sub region 24 h after the insult, revealed that 30 min OGD produced PI fluorescence levels that were 57 ± 8% of those observed when neuronal injury was maximal (Fig. 5). Compound **8** (1 μM) significantly reduced (29 ± 9%) the extent of OGD-induced neuronal death when added to the incubation medium during the 30 min insult and the subsequent 24 h recovery period (Fig. 5). Under the same experimental conditions, the AMPA receptor antagonist 2,3-dihydroxy-6-nitro-7-sulfamoyl-benzo[*f*] quinoxaline-2,3-dione (NBQX), at 30 μM concentration, dramatically reduced CA1 PI fluorescence levels (20 ± 4%). Fig. 5 also shows that compound **8** alone, at the concentration of 10 μM, was devoid of toxicity in slice cultures.

3.3.4. Electrophysiological studies in the CA1 region of rat acute hippocampal slices

Physiological functions of KA receptors are not fully understood yet and much attention has been paid to their role in ischemic brain injury. It is well known that KA receptors exert a variety of functions

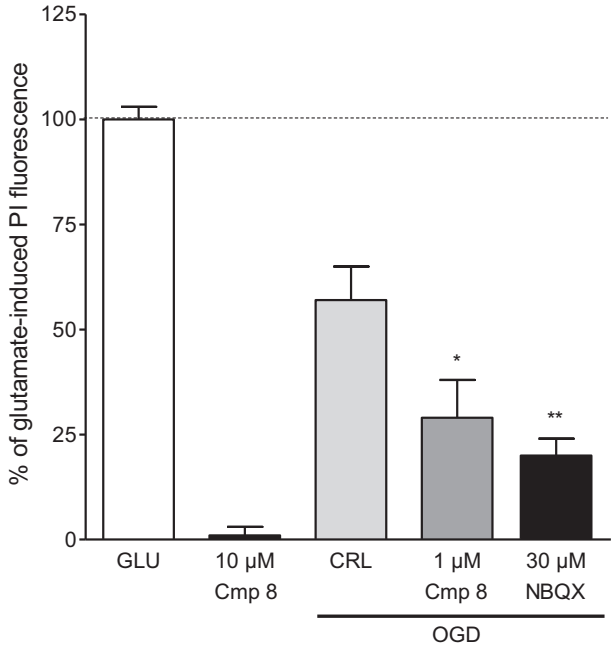

Fig. 5. Effect of compound (Cmp) **8** on OGD-induced neuronal damage in organotypic rat hippocampal slices. Hippocampal slices were exposed to 30 min OGD and 24 h later CA1 damage was assessed by measuring the intensity of PI fluorescence. Data are expressed as percent of maximal neuronal death, as measured following application of 10 mM glutamate (GLU) for 24 h. Background fluorescence was determined in control sister cultures not exposed to OGD and was subtracted from all experimental values. Each bar represents the mean ± S.E.M. of four experiments. $^{*}P < 0.05$ *vs* OGD (*t*-test + ANOVA); $^{**}P < 0.01$ *vs* OGD (*t*-test + ANOVA).

in the regulation of synaptic activity [28]. A considerable amount of data indicates that they are located both at the pre- and post-synaptic site and play a special role in regulating transmission and controlling short- and long-term plasticity in all subfields in the hippocampus [29–32]. On this basis, we decided to test at KA receptors the most active compound so far identified among the 3-hydroxyquinazoline-2,4-dione series, i.e. derivative **3**, to evaluate its effect on synaptic transmission in the CA1 region of acute isolated rat hippocampal slices, both under basal conditions and during OGD. Compound **3** possesses good affinity for high-affinity and low-affinity native KA receptors (K_i = 0.62 μM and 1.6 μM, respectively) (Table 1 and Ref. [18]). High-affinity and low-affinity native KA receptors consist of a combination of GluK4-5 [33–36] and GluK1-3 [35–37] subunits, respectively. Compound **3** also binds AMPA receptor with a K_i value of 16.5 μM.

In the first series of experiments we evaluated the efficacy of compound **3** in antagonizing the effect of kainate on field excitatory postsynaptic potential (fepsp) in the hippocampal CA1 region. In agreement with previous results [38–41], bath application of KA reversibly suppressed fepsp amplitude (Fig. 6A), thus inhibiting synaptic neurotransmission. It is known that this inhibitory effect of KA on fepsp is due to the stimulation of KA receptors located at presynaptic level in the CA1 region, thus inducing a decrease in glutamate release [39,42]. Kamiya and Ozawa [39] and Dargan et al. [42] have demonstrated that at low concentrations (0.5–1 μM), like those utilized in the present study, the fepsp suppression induced by KA, possibly by GLUK1 receptors, is not related i) to the activation of KA receptors located at postsynaptic levels; ii) to the activation of NMDA or AMPA receptors; or iii) to the effects of KA on inhibitory GABAergic neurotransmission. The inhibitory effect of KA on neurotransmission was antagonized by compound **3**. In fact, the KA-induced fepsp suppression was reduced by 1 μM compound

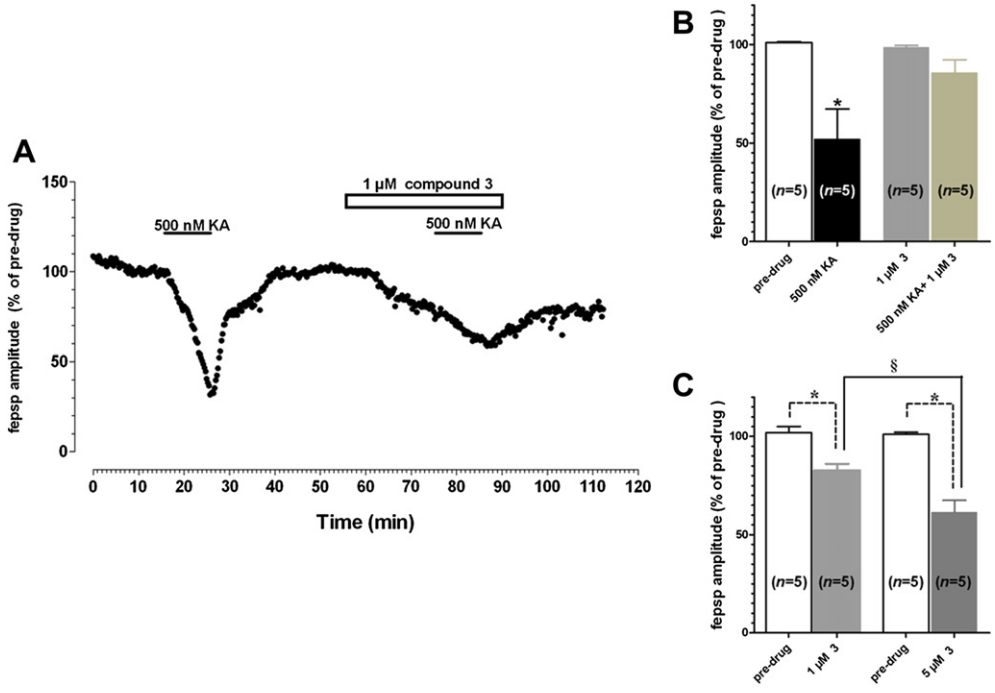

Fig. 6. Effect of compound **3** on KA-mediated suppression of excitatory transmission in the CA1 hippocampal region. Graph A shows the time course of fepsp amplitude recorded in a typical experiment before, during and after KA application (500 nM), in the absence or in the presence of 1 μM compound **3**. Data are expressed as percent of pre-drug. Closed bars indicate KA application; open bar indicates compound **3** application. Graph B displays the summary of results obtained in the presence of 500 nM KA, applied alone or in the presence of 1 μM compound **3**. Error bars are SEM; $^{*}p < 0.05$ paired Student's *t*-test *vs* respective pre-drug. Graph C shows the summary of the effects of compound **3**, applied at two different concentrations, on synaptic potentials under basal conditions. Error bars are SEM; $^{*}p < 0.05$ paired Student's *t*-test *vs* respective pre-drug; §$p < 0.05$ *vs* 1 μM compound **3**, One-way ANOVA followed by Newman–Keuls Multiple Comparison Test. The number of experiments are shown in parentheses.

3 (Fig. 6A). In particular, KA (500 nM, 10 min) suppressed fepsp amplitude to 52.1 ± 15.3% of the respective pre-drug ($p < 0.05$, $n = 5$) when applied alone, while in the presence of 1 μM compound **3** it suppressed fepsps to 85.8 ± 6.4% of the respective pre-drug level ($n = 5$) (Fig. 6B). Interestingly, compound **3** affected *per se* CA1 basal excitatory transmission (Fig. 6A and C). At a concentration of 1 μM, it reduced fepsp amplitude by 19.2 ± 3.2% ($p < 0.05$, $n = 6$) and at 5 μM by 39.6 ± 5.9% ($p < 0.05$, $n = 6$), in comparison to the respective controls (Fig. 6C). It is known that excitatory transmission in the CA1 region is due in large part to stimulation of AMPA receptors and that AMPA receptor antagonists suppress excitatory neurotransmission in this brain area where AMPA receptors are particularly abundant [43]. Our results, therefore, suggest that compound **3**, at the concentrations tested, also blocks native AMPA receptors.

Subsequently, the effect of compound **3** on neurotransmission was evaluated under ischemic conditions obtained, *in vitro*, by OGD application. In these experimental conditions, a severe, 7-min period of OGD always produced an irreversible and complete loss of synaptic transmission (Fig. 7A) and the appearance of anoxic depolarization (AD) in all slices examined (Fig. 7D). The loss of synaptic transmission is attributable to the massive release of

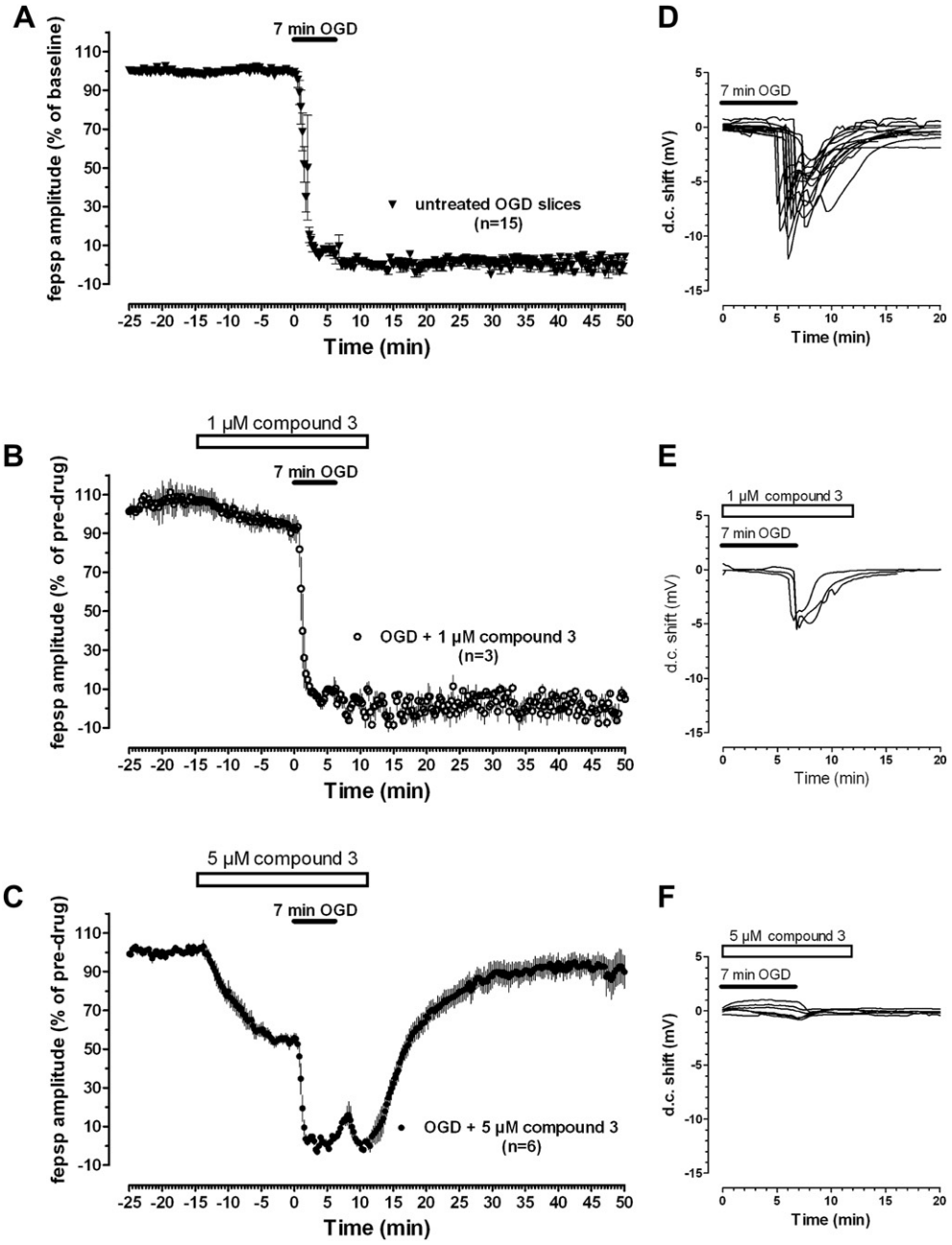

Fig. 7. Effect of compound **3** on the appearance of AD and the irreversible loss of neurotransmission induced by 7-min OGD in CA1 hippocampal slices (A–C). Each graph shows the time course of fepsp amplitude before, during 7-min OGD and after reperfusion in oxygenated aCSF in the absence (A) and in the presence of 1 μM compound **3** (B) or 5 μM compound **3** (C). Data are expressed as percent of pre-drug application (mean ± SEM). The number of slices are shown in parentheses. (D–F) AD was recorded as a negative voltage shift in response to 7-min OGD in the absence (D, $n = 15$) or in the presence of 1 μM compound **3** (E, $n = 3$) or 5 μM compound **3** (F, $n = 6$). The open bars show the application time of each drug. Closed bars indicate OGD time duration.

excitatory neurotransmitters [3]. AD, measured as negative direct current shift, is secondary to the strong depolarization induced by the OGD, and represents an important parameter of brain damage [44–48]. The direct current shift showed a mean peak latency of 6.45 ± 0.2 min ($n = 15$, calculated from the beginning of OGD) and a mean peak amplitude of 7.1 ± 0.5 mV ($n = 15$). The amplitude of fepsp did not recover (1.5 ± 1.8%, $n = 15$) when the slices were reperfused with oxygenated, glucose-containing artificial cerebrospinal fluid (aCSF) (Fig. 7A). Seven minutes of OGD was then applied in the presence of compound **3** which was superfused at two different concentrations (1 and 5 μM), 15 min before OGD induction. At 1 μM concentration it was unable to prevent the appearance of AD and the loss of neurotransmission induced by 7-min OGD ($n = 3$, Fig. 7B and E). Conversely, at 5 μM concentration, compound **3** prevented the appearance of AD in all slices tested ($n = 6$, Fig. 7F), allowing an almost complete recovery of fepsp amplitude (92.2 ± 4.4%; Fig. 7C). As previously described, compound **3** reduced fepsp amplitude under basal conditions (Fig. 7B and C, see also Fig. 6C).

In summary, compound **3**, applied at the concentration of 5 μM before, during and after a severe period of OGD allows a significant recovery of fepsp amplitude and prevents the appearance of AD.

This demonstrates that compound **3** is able to limit, during OGD, an excess of excitatory transmission which leads to excitotoxicity. We cannot exclude that the preventive effects of compound **3** on AD appearance and loss of neurotransmission induced by OGD could be related to the AMPA receptor blockade that was demonstrated to counteract AD appearance during OGD in hippocampal CA1 region [49]. Interestingly, specific antagonists of the KA receptor GluK2 subunit and of AMPA receptor are protective in cerebral ischemia models, both *in vivo* and *in vitro* [50–54].

4. Conclusion

The studies described in the present work have clarified the SARs of the 3-hydroxyquinazolin-2-4-dione series as iGluRs antagonists. Molecular modeling investigation has permitted prediction of the hypothetical binding mode of the new derivatives at the Gly/NMDA and AMPA receptors and rationalization of affinity and selectivity profiles of some derivatives.

Some new Gly/NMDA and AMPA receptor antagonists were identified and the most potent at the AMPA receptor was the 6-(1,2,4-triazol-yl)-substituted compound **8**. This derivative demonstrated efficacy both in counteracting neuronal damage in organotypic rat hippocampal slices exposed to OGD and as anticonvulsant agent. Compound **3**, possessing the highest KA receptor affinity and selectivity among the 3-hydroxyquinazolin-2,4-dione series, showed neuroprotective properties in an *in vitro* electrophysiological model of cerebral ischemia. In fact, it was effective in preventing both the failure of synaptic activity and the appearance of AD induced by OGD.

5. Experimental section

5.1. Chemistry

Silica gel plates (Merck F254) and silica gel 60 (Merck, 70-230 mesh) were used for analytical and column chromatography, respectively. All melting points were determined on a Gallenkamp melting point apparatus and are uncorrected. Microanalyses were performed with a Perkin–Elmer 260 elemental analyzer for C, H, N, and the results were within ±0.4% of the theoretical values, unless otherwise stated. The IR spectra were recorded with a Perkin–Elmer Spectrum RX I spectrometer in Nujol mulls and are expressed in cm^{-1}. NMR spectra were recorded on a Brucker Avance 400 spectrometer (400 MHz for ^1H NMR, 100 MHz for ^{13}C NMR). The chemical shifts are reported in δ (ppm) and are relative to the central peak of the solvent which was always DMSO-d_6. The following abbreviations are used: s = singlet, d = doublet, t = triplet, m = multiplet, br = broad, and ar = aromatic protons. ^{13}C NMR signals are singlets, unless otherwise stated.

5.1.1. 2-Amino-N-(benzyloxy)-4-trifluoromethylbenzamide (**13**)

Triethylamine (4.3 mmol) was added to a suspension of O-benzylhydroxylamine hydrochloride (4.3 mmol) in ethanol (15 mL). The 7-trifluoromethyl-1,2-dihydro-3,1-benzoxazine-2,4-dione **13** [21] (4.3 mmol) was added to the solution and the mixture was heated at reflux for 3 h. Cooling at room temperature and dilution with water (about 50 mL) gave a solid that was collected, washed with water and recrystallized. Yield: 90%; mp 146–148 °C (cyclohexane) ^1H NMR: 4.88 (s, 2H, CH_2), 6.55 (br s, 2H, NH_2) 6.75 (d, 1H, ar, $J = 7.7$ Hz), 7.00 (s, 1H, ar), 7.33–7.39 (m, 6H, ar), 11.70 (s, 1H, NH) Anal. Calcd for: $C_{15}H_{13}F_3N_2O_2$: C, 58.07; H, 4.22; N, 9.03. Found: C, 57.96; H, 4.41; N, 9.31.

5.1.2. 3-Benzyloxy-7-trifluoromethyl-1H-quinazoline-2,4-dione (**14**)

Triethylamine (7.7 mol) was dropwise added to a solution of compound **13** (3.2 mmol) and triphosgene (1.28 mmol) in anhydrous tetrahydrofuran (30 mL). The mixture was stirred at room temperature for about 1 h then diluted with water (80 mL) to give a solid which was collected, washed with water and recrystallized. Yield: 92%; mp 228–230 °C (cyclohexane) ^1H NMR: 5.09 (s, 2H, CH_2), 7.39–7.56 (m, 7H, ar), 8.15 (d, 1H, ar, $J = 8.4$ Hz), 11.93 (s, 1H, NH). Anal. Calcd for $C_{16}H_{11}F_3N_2O_3$: C, 57.15; H, 3.30; N, 8.33. Found: C, 57.38; H, 3.01; N, 8.62.

5.1.3. 7-Trifluoromethyl-3-hydroxy-1H-quinazoline-2,4-dione (**4**)

A suspension of compound **14** (3.3 mmol) in 48% hydrobromic acid (6 mL) and glacial acetic acid (6 mL) was refluxed for about 3 h. The resulting solution was cooled at room temperature and diluted with water (50 mL), the solid was collected, washed with water and recrystallized. Yield: 95%; mp 256–257 °C (cyclohexane/EtOAc). ^1H NMR: 7.46 (s, 1H, ar), 7.51 (d, 1H, ar, $J = 8.0$ Hz), 8.12 (d, 1H, ar, $J = 8.0$ Hz), 10.80 (s, 1H, OH), 11.80 (s, 1H, NH). ^{13}C NMR: 112.74, 117.74, 118.91, 125.15 (q, CF_3), 129.30 (C5), 134.41 (q, C7), 139.15, 148.97 (C2), 159.04 (C4). IR 1670, 1750, 3480. Anal. Calcd for $C_9H_5F_3N_2O_3$: C, 43.92; H, 2.05; N, 11.38. Found: C, 43.78; H, 1.95; N, 11.02.

5.1.4. 3-Acetoxy-7-trifluoromethyl-1H-quinazoline-2,4-dione (**15**)

A suspension of derivative **4** (1.4 mmol) in acetic anhydride (15 mL) was refluxed for 2 h. Evaporation of the excess of acetic anhydride at reduced pressure gave a residue that was stirred with water (40 mL). The solid obtained was collected, washed with water and recrystallized. Yield: 85%; mp 245–246 °C (cyclohexane/EtOAc). ^1H NMR: 2.38 (s, 3H, CH_3), 7.50 (s, 1H, ar), 7.58 (d, 1H, ar, $J = 8.0$ Hz), 8.15 (d, 1H, ar, $J = 8.0$ Hz), 12.20 (br s, 1H, NH). ^{13}C NMR: 17.79 (CH_3), 113.28, 117.23, 119.59, 123.58 (q, CF_3), 129.45 (C5), 135.21 (q, C_7), 139.60, 146.85 (C2), 157.31 (C4), 167.36 (acetoxy CO). Anal. Calcd for $C_{11}H_7F_3N_2O_4$: C, 45.85; H, 2.45; N, 9.72. Found: C, 45.66; H, 2.23; N, 9.63.

5.1.5. 3-Acetoxy-7-trifluoromethyl-6-nitro-1H-quinazoline-2,4-dione (**16**)

Compound **15** (4.0 mmol) was portionwise added to cooled (−10 °C) HNO_3 (90%, 14 mL). When the addition was completed (1 h), the mixture was stirred for about 30 min at 0 °C, then the solution was poured onto ice (about 100 g) and the solid collected,

washed with abundant water and recrystallized. Yield: 82%; mp 252–254 °C (EtOH). ^{1}H NMR: 2.42 (s, 3H, CH_3), 7.73 (s, 1H, ar), 8.67 (s, 1H, ar), 12.72 (br s, 1H, NH). Anal. Calcd for $C_{11}H_6F_3N_3O_6$: C, 39.65; H, 1.82; N, 12.61. Found: C, 41.56; H, 1.99; N, 10.43.

*5.1.6. 6-Amino-3-acetoxy-7-trifluoromethyl-1H-quinazoline-2,4-dione (**17**)*

20% Pd/C was added to a solution of compound **16** (1.7 mmol) in ethanol (200 mL) and the mixture was hydrogenated in a Parr apparatus at 40 psi for 24 h. The catalyst was filtered off and the solvent evaporated at reduced pressure to yield a solid that was recrystallized. Yield: 80%; mp 266–267 °C (EtOAc). ^{1}H NMR: 2.37 (s, 3H, CH_3), 5.73 (s, 2H, NH_2), 7.27 (s, 1H, ar), 7.45 (s, 1H, ar), 12.00 (br s, 1H, NH). Anal. Calcd for $C_{11}H_8F_3N_3O_4$: C, 43.58; H, 2.66; N, 13.86. Found: C, 43.71; H, 1.95; N, 14.59.

*5.1.7. 6-(2-Carboxybenzoylamino)-7-trifluoromethyl-3-hydroxy-1H-quinazoline-2,4-dione (**7**)*

A mixture of the 6-amino derivative **17** (1.1 mmol), phthalic anhydride (3.3 mmol) and sodium acetate (1.1 mmol) in glacial acetic acid (5 mL) was heated at 60 °C for about 36 h. After cooling at room temperature, the suspension was diluted with water (30 mL) and acidified to pH 4 with 6 N HCl. The solid which precipitated was collected and suspended in 0.25 M NaOH solution (4 mL). The mixture was stirred at room temperature for 30 min, then the solution acidified to pH = 1 with 6 N HCl, the solid collected, washed with water and recrystallized. Yield: 35%; mp >300 °C (EtOH); ^{1}H NMR: 7.44 (d, 1H, ar, J = 7.4 Hz), 7.54 (s, 1H, ar), 7.57–7.71 (m, 3H, ar), 8.14 (d, 1H, ar, J = 7.59), 10.10 (s, 1H, OH or NH), 11.39 (s, 1H, OH or NH), 11.58 (s, 1H, NH or OH), 13.24 (br s, 1H, COOH); IR 1698, 1728, 2500–3300. Anal. Calcd for $C_{17}H_{10}F_3N_3O_6$: C, 49.89; H, 2.46; N, 10.27. Found: C, 49.61; H, 2.25; N, 10.39.

*5.1.8. 2-Amino-N-methoxy-4-trifluoromethylbenzamide (**18**)*

Triethylamine (2.16 mmol) was added to a suspension of O-methylhydroxylamine hydrochloride (2.16 mmol) in ethanol (10 mL). The 7-trifluoromethyl-1,2-dihydro-3,1-benzoxazine-2,4-dione **12** [21] (2.16 mmol) was added to the solution and the mixture was heated at reflux for about 2 h. The solution was cooled at room temperature and concentrated to small volume by evaporation of the solvent at reduced pressure. Dilution with water (about 80 mL) gave a solid that was collected, washed with water and recrystallized. Yield: 85%; mp 165–167 °C (cyclohexane/EtOAc) ^{1}H NMR: 3.69 (s, 3H, CH_3), 6.58 (br s, 2H, NH_2) 6.78 (d, 1H, ar, J = 8.1 Hz), 7.06 (s, 1H, ar), 7.47 (d, 1H, ar, J = 8.1 Hz), 11.63 (s, 1H, NH). IR 1648, 3197, 3382, 3489. Anal. Calcd for $C_9H_9F_3N_2O_2$: C, 46.16; H, 3.87; N, 11.96. Found: C, 46.01; H, 4.09; N, 10.89.

*5.1.9. 3-Methoxy-7-trifluoromethyl-1H-quinazoline-2,4-dione (**19**)*

Triethylamine (5.1 mol) was dropwise added to a solution of compound **18** (2.1 mmol) and triphosgene (0.85 mmol) in anhydrous tetrahydrofuran (30 mL). The mixture was stirred at room temperature for about 2 h then diluted with water (100 mL) and extracted with EtOAc (60 mL for three times). The organic layers were anhydrified (Na_2SO_4) and the solvent evaporated at reduced pressure. The obtained oil was treated with diethyl ether to give a solid that was collected and recrystallized. Yield: 65%; mp 220–223 °C (EtOH) ^{1}H NMR: 3.89 (s, 3H, CH_3), 7.48 (s, 1H, ar), 7.55 (d, 1H, ar, J = 8. 1 Hz), 8.15 (d, 1H, ar, J = 8.1 Hz), 11.86 (s, 1H, NH). ^{13}C NMR: 64.08 (OCH_3), 112.73, 117.97, 118.80 (C8), 123.64 (q, CF_3), 129.24 (C5), 134.63 (q, C7), 139.40, 147.92, 158.31. IR 1726, 1759, 3567. Anal. Calcd for $C_{10}H_7F_3N_2O_3$: C, 46.16; H, 2.71; N, 10.77. Found: C, 46.38; H, 2.92; N, 10.54.

*5.1.10. 3-Methoxy-7-trifluoromethyl-6-nitro-1H-quinazoline-2,4-dione (**20**)*

Compound **18** (4.6 mmol) was portionwise added to cooled (−10 °C) HNO_3 (90%, 15 mL). After the addition was completed (1 h), the mixture was stirred for about 1 h and 30 min, then the solution was poured onto ice (about 100 g). The mixture was extracted with EtOAc (60 mL for three times), the organic layers were dried (Na_2SO_4) and the solvent evaporated at reduced pressure to yield a solid that was collected by filtration and recrystallized. Yield: 80%; mp 220–222 °C (EtOH). ^{1}H NMR: 3.91 (s, 3H, CH_3), 7.67 (s, 1H, ar), 8.64 (s, 1H, ar), 12.36 (br s, 1H, NH). ^{13}C NMR: 64.03 (OCH_3), 116.36 (C8), 117.82, 121.9 (q, CF_3), 126.64 (C5), 127.40 (q, C7), 141.28, 142.44, 148.15 (C2), 157.69 (C4). Anal. Calcd for $C_{10}H_6F_3N_3O_5$: C, 39.36; H, 1.98; N, 13.77. Found: C, 39.54; H, 1.67; N, 13.94.

*5.1.11. 6-Amino-3-methoxy-7-trifluoromethyl-1H-quinazoline-2,4-dione (**21**)*

A mixture of compound **20** (3.4 mmol) and Pd/C (10%, 0.2 g) in EtOH (100 mL) was hydrogenated at 40 psi in a Parr apparatus for 14 h. The catalyst was filtered off and the solvent evaporated at reduced pressure to give a solid that was collected and recrystallized. Yield: 82%; mp 250–252 °C (EtOH). ^{1}H NMR: 3.86 (s, 3H, CH_3), 5.65 (br s, 2H, NH_2), 7.23 (s, 1H, ar), 7.47 (s, 1H, ar), 11.36 (s, 1H, NH). IR 1697, 1718, 1747, 3151, 3185. Anal. Calcd for $C_{10}H_8F_3N_3O_3$: C, 43.65; H, 2.93; N, 15.27. Found: C, 43.89; H, 2.68; N, 15.01.

*5.1.12. 3-Methoxy-7-trifluoromethyl-6-(1,2,4-triazol-4-yl)-1H-quinazoline-2,4-dione (**22**)*

Diformylhydrazine (3.3 mmol) and then, drop by drop, trimethylsilylchloride (16.5 mmol) were added to a solution of compound **21** (1.1 mmol) in anhydrous pyridine (5 mL). The mixture was heated at 100 °C for 24 h, then the solvent evaporated at reduced pressure. The residue was treated with water (5–10 mL) and extracted with EtOAc (20 mL for three times). Evaporation of the dried (Na_2SO_4) organic layers afforded a solid which was collected and recrystallized. Yield: 90%; mp >300 °C (MeOH). ^{1}H NMR: 3.91 (s, 3H, CH_3), 7.67 (s, 1H, ar), 8.20 (s, 1H, ar), 8.79 (s, 2H, triazole protons), 12.15 (br s, 1H, NH). IR 1697, 1745, 3121. Anal. Calcd for $C_{12}H_8F_3N_5O_3$: C, 44.05; H, 2.46; N, 21.40. Found: C, 44.24; H, 2.39; N, 21.25.

*5.1.13. 7-Trifluoromethyl-3-hydroxy-6-nitro-1H-quinazoline-2,4-dione (**5**)*

A solution of compound **20** (2.9 mmol) in 48% HBr (18 mL) and glacial acetic acid (18 mL) was refluxed for about 48 h. The solution was concentrated to small volume, diluted with water (about 60 mL) and extracted with EtOAc (50 mL for three times). Evaporation of the dried (Na_2SO_4) organic layers afforded a solid which was collected and recrystallized. Yield: 53%; mp 229–231 °C (EtOH). ^{1}H NMR: 7.64 (s, 1H, ar), 8.60 (s, 1H, ar), 11.02 (br s, 1H, OH), 12.30 (br s, 1H, NH). ^{13}C NMR: 116.5 (C8), 117.36, 121.91 (q, CF_3), 126.58 (C5), 127.10 (q, C7), 141.03, 142.36, 148.73 (C2), 157.90 (C4). Anal. Calcd for $C_9H_4F_3N_3O_5$: C, 37.13; H, 1.38; N, 14.43. Found: C, 38.86; H, 1.59; N, 16.33.

*5.1.14. 6-Amino-7-trifluoromethyl-3-hydroxy-1H-quinazoline-2,4-dione (**6**)*

20% Pd/C was added to a solution of compound **5** (1.7 mmol) in ethanol (200 mL) and the mixture was hydrogenated in a Parr apparatus at 40 psi for 24 h. The catalyst was filtered off and the solvent evaporated at reduce pressure to yield a solid that was recrystallized. Yield: 85%; mp 290–292 °C (EtOAc). ^{1}H NMR: 5.59 (s, 2H, NH_2), 7.22 (s, 1H, ar), 7.43 (s, 1H, ar), 10.60 (br s, 1H, OH or NH), 11.20 (br s, 1H, NH or OH). IR 1670, 1735, 3390–3420. Anal.

Calcd for $C_9H_6F_3N_3O_3$: C, 41.39; H, 2.32; N, 16.09. Found: C, 42.91; H, 2.06; N, 16.29.

5.1.15. 7-Trifluoromethyl-3-hydroxy-6-(1,2,4-triazol-4-yl)-1H-quinazoline-2,4-dione (**8**)

The title compound was obtained by reacting derivative **6** (3.3 mmol) with diformylhydrazine (3.3 mmol) in the same conditions described above to prepare compound **22** from **21**. Yield: 85%; mp >300 °C (EtOH). ^{1}H NMR: 7.65 (s, 1H, ar), 8.13 (s, 1H, ar), 8.76 (s, 2H, triazole protons), 10.70 (br s, 1H, OH or NH), 12.00 (br s, 1H, NH or OH). ^{13}C NMR: 115.20 (C8), 117.88, 122.45 (q, CF_3), 125.31, 129.68 (C5), 130.65 (C7), 139.83, 144.42 (C triazole), 148.87 (C2), 158.29 (C4). IR 1683, 1734, 3506. Anal. Calcd for $C_{11}H_6F_3N_5O_3$: C, 42.18; H, 1.93; N, 22.36. Found: C, 42.24; H, 2.09; N, 22.65.

5.1.16. 7-Trifluoromethyl-3-hydroxy-6-(pyrrol-1-yl)-1H-quinazoline-2,4-dione (**9**)

A solution of 2,5-diethoxytetrahydrofuran (3.6 mmol) in glacial acetic acid (3 mL) was dropwise added to a hot (90 °C) suspension of the 6-amino-derivative **6** (1.2 mmol) in glacial acetic acid (8 mL). The solution was heated at 90 °C for 25 min, then the solvent was distilled off at reduced pressure. The tarry residue was treated with water and the solid collected and recrystallized. Yield: 84%; mp 280–282 °C (EtOH); ^{1}H NMR: 6.24 (s, 2H, pyrrole protons), 6.92 (s, 2H, pyrrole protons), 7.61 (s, 1H, ar), 7.77 (s, 1H, ar), 11.54 (br s, 1H, NH or OH), 11.70 (br s, 1H, NH or OH). IR 1690, 1708, 1734, 3178. Anal. Calcd for $C_{13}H_8F_3N_3O_3$: C, 50.17; H, 2.59; N, 13.50. Found: C, 52.29; H, 2.38; N, 13.79.

5.1.17. 7-Trifluoromethyl-3-hydroxy-6-(3-formylpyrrol-1-yl)-1H-quinazoline-2,4-dione (**10**)

A solution of 2,5-dimethoxytetrahydrofuran-3-carbaldehyde (2.8 mmol) in glacial acetic acid (7 mL) was dropwise added to a hot (90 °C) suspension of the 6-amino-derivative **6** (1.9 mmol) in glacial acetic acid (8 mL). After the addition was completed, the mixture was stirred at room temperature for 30 min. Evaporation of the solvent at reduced pressure yielded a solid which was suspended in water (10–20 mL), collected and recrystallized. Yield: 83%; mp 280–282 °C (EtOH); ^{1}H NMR: 6.65 (s, 1H, pyrrole protons), 7.11 (s, 1H, pyrrole proton), 7.65 (s, 1H, ar), 7.87 (s, 1H, pyrrole proton), 7.98 (s, 1H, ar), 9.77 (s, 1H, CHO), 10.94 (br s, 1H, OH or NH), 12.05 (br s, 1H, NH or OH); IR 1656, 1687, 1736, 3125, 3250. Anal. Calcd for $C_{14}H_8F_3N_3O_4$: C, 49.57; H, 2.38; N, 12.39. Found: C, 49.81; H, 2.26; N, 12.53.

5.1.18. 7-Trifluoromethyl-3-hydroxy-6-(3-carboxypyrrol-1-yl)-1H-quinazoline-2,4-dione (**11**)

Potassium permanganate (0.67 g) was portionwise added to a cooled (0 °C) suspension of compound **10** (1.54 mmol) in a 1:1 acetone/water mixture (10 mL). Each small addition was made after the disappearance of the violet color of the oxidizing agent. After the additions were completed, the mixture was stirred at room temperature for 1 h and 30 min, then the excess of potassium permanganate was quenched with a 38% solution of sodium hydrogen sulfite and the solution acidified with 6 N HCl. The solid was collected, washed with water and recrystallized. Yield: 75%; mp 210–212 °C (Cyclohexane/EtOAc); ^{1}H NMR: 6.57 (s, 1H, pyrrole proton), 7.02 (s, 1H, pyrrole proton), 7.52 (s, 1H, ar), 7.65 (s, 1H, pyrrole proton), 7.94 (s, 1H, ar), 10.92 (s, 1H, OH or NH), 12.02 (s, 1H, NH or OH), 12.07 (br s, 1H, COOH). ^{13}C NMR: 110.68 (C pyrrole), 115,09 (C8), 117.79, 118.02, 122.80 (q CF_3), 125.79 (C pyrrole), 129.07 (C5 and C pyrrole), 130.69 (q C7), 131.61, 138.96, 148.88 (C2), 158.38 (C4), 165.60 (COOH). IR 1680, 1740, 3100–3200. Anal. Calcd for $C_{14}H_8F_3N_3O_5$: C, 47.34; H, 2.27; N, 11.83. Found: C, 47.07; H, 2.02; N, 11.61.

5.2. Molecular modeling studies

5.2.1. Target structures

The crystal structures of AMPA and Glycine/NMDA receptor subunit were retrieved from the PDB (PDB code: 3R7X and 1PBQ, respectively) [24,55]. Hydrogen atoms were added using standard geometries to the protein structure with the Molecular Operation Environment (MOE, version 2010.11) program [56]. To appropriately assign ionization states and hydrogen positions, the "Protonate-3D" tool implemented by MOE [57,58] was used. To minimize contacts among hydrogens, the structures were subjected to Amber94 [5] force field minimization until the *rms* of conjugate gradient was <0.05 kcal/mol/Å, keeping the heavy atoms fixed at their crystallographic positions.

5.2.2. Molecular docking protocol

All docked ligands were built using the "Builder" module of MOE [55]. Ligands were docked into the putative binding sites using GOLD 5.0 suite [59]. Charges for ligands were imported from the MOPAC program output files using PM3/ESP semiempirical Hamiltonian [60,61]. The genetic algorithm implemented by GOLD performs 25 independent docking runs and writes the resulting conformations and their energies in a molecular database file. The top ranking pose for each compound was selected according to the scaffold orientation of a quinazolinedione sulfonamide derivative, which has been recently co-crystallized by M. Koller and co-workers [24].

5.3. Pharmacology

All animal procedures were conducted according to the Italian Guidelines for Animal Care, DL 116/92, application of the European Communities Council Directive (86/609/EEC).

5.3.1. Binding assay

Rat cortical synaptic membrane preparation [^{3}H]glycine (53 Ci/mmol), [^{3}H]AMPA (66 Ci/mmol), and [^{3}H]-(+)-MK-801 (22.5 Ci/mmol) binding experiments were performed following the procedure reported in Refs. [12,62] and [19] respectively. The high affinity [^{3}H]kainate (58 Ci/mmol), binding assays were performed on rat cortical membrane, according to a previously described method [16].

5.3.2. Functional antagonism studies at AMPA and NMDA sites

The mouse cortical wedge preparation described by Mannaioni et al. [63] was used, while the electrophysiological assays were performed following the procedures described in Ref. [14].

5.3.3. Sample preparation and result calculation

A stock 1 mM solution of the tested compound was prepared in 50% DMSO and the subsequent dilution was accomplished in buffer. The IC_{50} values were calculated from three or four displacement curves based on four to six scalar concentrations of the tested compound in triplicate using the ALLFIT computer program [64]. K_i values were calculated according to the Cheng–Prusoff equation [65]. Under our experimental conditions, the dissociation constant (K_D) for [^{3}H]glycine and [^{3}H]-DL-AMPA were 75 ± 6 and 28 ± 3 nM, respectively.

5.3.4. Oxygen–glucose deprivation (OGD) in rat organotypic hippocampal slice cultures

Organotypic hippocampal slice cultures were prepared from seven-day-old Wistar rats, used at 14 DIV (days *in vitro*) and exposed to OGD as previously described [26]. Briefly, the slices were preincubated for 30 min in serum-free medium and then

subjected to OGD by exposing them to a serum-free medium devoid of glucose and previously saturated with 95% N_2/5% CO_2. Following 30 min incubation at 37 °C in an airtight anoxic chamber, the cultures were transferred to oxygenated serum-free medium containing 5 mg/mL glucose and 5 μg/mL propidium iodide (PI) and returned to the incubator under normoxic conditions until neuronal injury was evaluated 24 h later. In this system, 30-min OGD induced a CA1 pyramidal cell damage that was approximately 65% of the maximal damage achieved by exposing the slices for 24 h to 10 mM glutamate. Test compounds were added to cultures during OGD and maintained for the subsequent 24 h. A stock 1 mM solution of compound **8** was prepared in 50% DMSO and the subsequent dilution was accomplished in buffer.

Cell injury in the CA1 hippocampal region, was assessed according to Ref. [26], using PI, a polar dye which enters the cells only if the membrane is damaged and becomes fluorescent upon binding to DNA. Background PI fluorescence was determined in control cultures not exposed to OGD and was subtracted to all experimental values. There was a linear correlation between CA1 PI fluorescence intensity and the number of injured CA1 pyramidal cells as detected by morphological criteria.

5.3.5. Oxygen–glucose deprivation (OGD) in rat acute hippocampal slices

5.3.5.1. Electrophysiology. Experiments were carried out on acute hippocampal slices as previously described [44]. Briefly, male Wistar rats (Harlan, Udine, Italy, 1-2 month-old) were killed under isoflurane-induced anesthesia and their hippocampi were rapidly removed and placed in ice-cold oxygenated (95% O_2–5% CO_2) artificial cerebrospinal fluid (aCSF). Rat brains and slices were maintained in aCSF containing (in mM): NaCl 125, KCl 3, NaH_2PO_4 1.25, $MgSO_4$ 1, $CaCl_2$ 2, $NaHCO_3$ 25 and D-glucose 10. Parasagittal rat hippocampal slices (400 μm thick) were prepared using a McIlwain tissue chopper (The Mickle Lab. Engineering, Co. Ltd., Gomshall, UK) and kept in oxygenated aCSF for at least 1 h at room temperature. A single slice was then placed on a nylon mesh in a small chamber (0.8 mL), completely submerged and superfused with oxygenated aCSF (31–32 °C) at a constant flow rate of 1.5–1.8 mL/min. Test pulses (100 μs, 0.066 Hz) were delivered through a bipolar nichrome electrode positioned in the CA1 stratum radiatum in order to stimulate Schaffer collateral/commissural fibers. Evoked extracellular fepsps were recorded with glass microelectrodes (2–10 MΩ, Harvard Apparatus LTD, Edenbridge, UK) filled with 150 mM NaCl and placed in the stratum radiatum of the CA1 hippocampal region. Responses were amplified (BM 622, Mangoni, Pisa, Italy), digitized (sample rate, 33.33 kHz), and stored for later analysis with LTP (version 2.30D) program [66].

Stimulus–response curves were obtained by gradually increasing stimulus strength at the beginning of each experiment, until a stable baseline of evoked response was reached. The test stimulus pulse was then adjusted to produce a fepsp, whose slope and amplitude was 40–50% of the maximum and was kept constant throughout the experiment. The fepsp amplitude was routinely measured, and expressed as the percentage of the average amplitude of the potentials measured during the 5-min preceding exposure of the hippocampal slices to drug treatment (pre-drug) or OGD (pre-ischemic).

5.3.5.2. Application of OGD and drugs in rat acute hippocampal slices. OGD was obtained by superfusing the slice with aCSF without glucose and gassed with nitrogen (95% N_2 -5% CO_2) [67]. This caused a drop in pO_2 in the recording chamber from ~500 mm Hg (normoxia) to a range of 35–75 mm Hg (after 7-min OGD) [44]. At the end of the ischemic period, the slice was again superfused with normal, glucose containing, oxygenated aCSF.

All drugs were stored at −20 °C in stock solutions at 1000–10,000 times the desired final concentration, dissolved in aCSF and applied to the slice by superfusion. Compound **3** was dissolved in dimethylsulfoxide (DMSO) and stock solutions were made to obtain concentrations of DMSO lower than 0.001% in the superfusing aCSF. Control experiments, carried out in parallel, showed that this concentration of DMSO did not affect CA1 hippocampal neurotransmission. Changes in superfusing solutions reached the preparation in 60 s and this delay was taken into account in our calculations.

5.3.5.3. Data analysis. Data were analyzed using WinLTP 1.11 reanalysis program and the software package GRAPHPAD PRISM (version 4.0; GraphPad Software, San Diego, CA, USA). All numerical data are expressed as mean ± SEM. Statistical significance was evaluated using paired two-tailed Student's *t*-test and One-way ANOVA. Differences were considered significant at $p < 0.05$.

5.3.6. Anticonvulsant studies

Male Swiss albino mice (23–30 g) from Harlan (Varese) breeding farm were used. Fifteen mice were housed per cage. The cages were placed in the experimental room 24 h before the test for acclimatization. The animals were kept at 23 ± 1 °C with a 12 h light/dark cycle, light at 7 a.m., with food and water ad libitum.

Drugs: Diazepam (Valium 10 – Roche), Pentylenetetrazole (PTZ) (Sigma). PTZ was dissolved in isotonic (0.9% NaCl) saline solution and injected by the s.c. route. Compound **8** was dispersed in 1% sodium carboxymethylcellulose (CMC) immediately before use. Drug concentrations were prepared in such a way that the necessary dose could be administered in a volume of 10 ml kg^{-1} by the p.o route. PTZ (90 mg/kg s.c.) was injected 30 min after the administration of drugs. The frequency of the occurrence of clonic generalized convulsions was noted over a period of 30 min.

Acknowledgements

The synthetic work was supported by a grant of the University of Florence and the Italian Ministry for University and Research, Italy. The molecular modeling work coordinated by S.M. has been carried out with financial support from the University of Padova, Italy, and the Italian Ministry for University and Research, Rome, Italy.

References

[1] H. Bräuner-Osborne, J. Egebjerg, E.Ø. Nielsen, U. Madsen, P. Krogsgaard-Larsen, J. Med. Chem. 43 (2000) 2609–2654.
[2] S.F. Traynelis, L.P. Wollmuth, C.J. McBain, F.S. Menniti, K.M. Vance, K.K. Odgen, K.B. Hansen, H. Yuan, S.J. Myers, R. Dingledine, Pharmacol. Rev. 62 (2010) 405–496.
[3] G.G. Somjen, Physiol. Rev. 81 (2001) 1065–1096.
[4] M.R. Hynd, H.L. Scott, P.R. Dodd, Neurochem. Int. 45 (2004) 583–595.
[5] W.M. Caudle, J. Zhang, Exp. Neurol. 220 (2009) 230–233.
[6] J.C. Corona, L.B. Tovar-y-Romo, R. Tapia, Expert Opin. Ther. Targets 11 (2007) 1415–1428.
[7] M.A. Rogawski, Epilepsy Currents 11 (2011) 56–63.
[8] N.G. Walgren, Int. Rev. Neurobiol. 40 (1997) 337–363.
[9] K.W. Muir, Curr. Opin. Pharmacol. 6 (2006) 53–60.
[10] V. Colotta, D. Catarzi, F. Varano, L. Cecchi, G. Filacchioni, A. Galli, C. Costagli, Arch. Pharm. Pharm. Med. Chem. 330 (1997) 129–134.
[11] D. Catarzi, V. Colotta, F. Varano, L. Cecchi, G. Filacchioni, A. Galli, C. Costagli, J. Med. Chem. 42 (1999) 2478–2484.
[12] D. Catarzi, V. Colotta, F. Varano, L. Cecchi, G. Filacchioni, A. Galli, C. Costagli, V. Carlà, J. Med. Chem. 43 (2000) 3824–3826.
[13] D. Catarzi, V. Colotta, F. Varano, L. Cecchi, G. Filacchioni, A. Galli, C. Costagli, V. Carlà, J. Med. Chem. 44 (2001) 3157–3165.
[14] F. Varano, D. Catarzi, V. Colotta, G. Filacchioni, A. Galli, C. Costagli, V. Carlà, J. Med. Chem. 44 (2002) 1035–1044.
[15] V. Colotta, D. Catarzi, F. Varano, F.R. Calabri, G. Filacchioni, C. Costagli, A. Galli, Bioorg. Med. Chem. Lett. 14 (2004) 2345–2349.
[16] D. Catarzi, V. Colotta, F. Varano, F.R. Calabri, G. Filacchioni, A. Galli, C. Costagli, V. Carlà, J. Med. Chem. 47 (2004) 262–272.

[17] F. Varano, D. Catarzi, V. Colotta, F.R. Calabri, O. Lenzi, G. Filacchioni, A. Galli, C. Costagli, F. Deflorian, S. Moro, Bioorg. Med. Chem. 13 (2005) 5536–5549.
[18] V. Colotta, D. Catarzi, F. Varano, O. Lenzi, G. Filacchioni, C. Costagli, A. Galli, C. Ghelardini, N. Galeotti, P. Gratteri, J. Sgrignani, F. Deflorian, S. Moro, J. Med. Chem. 49 (2006) 6015–6026.
[19] F. Varano, D. Catarzi, V. Colotta, L. Cecchi, G. Filacchioni, A. Galli, C. Costagli, Eur. J. Med. Chem. 36 (2001) 203–209.
[20] D. Catarzi, O. Lenzi, V. Colotta, F. Varano, D. Poli, G. Filacchioni, K. Lingenhöhl, S. Ofner, Chem. Pharm. Bull. 58 (2010) 908–911.
[21] F.R. Calabri, V. Colotta, D. Catarzi, F. Varano, O. Lenzi, G. Filacchioni, C. Costagli, A. Galli, Eur. J. Med. Chem. 40 (2005) 897–907.
[22] P.D. Leeson, L.L. Iversen, J. Med. Chem. 37 (1994) 4053–4067.
[23] C.F. Bigge, S.S. Nikam, Exp. Opin. Ther. Pat. 7 (1997) 1099–1114.
[24] M. Koller, K. Lingenhoehl, M. Schmutz, I.-T. Vranesic, J. Kallen, Y.P. Auberson, D.A. Carcache, H. Mattes, S. Ofner, D. Orain, S. Urwyler, Bioorg. Med. Chem. Lett. 21 (2011) 3358–3361.
[25] StarDrop. Optibrium Ltd., 7226 IQ Cambridge, Beach Drive, Cambridge, CB25 9TL, UK. http://www.optibrium.com/.
[26] D.E. Pellegrini-Giampietro, A. Cozzi, F. Peruginelli, P. Leonardi, E. Meli, R. Pellicciari, F. Moroni, Eur. J. Neurosci. 11 (1999) 3637–3647.
[27] M. Montero, M. Nielsen, L.C.B. Rønn, A. Møller, J. Noraberg, J. Zimmer, Brain Res. 1177 (2007) 124–135.
[28] G.L. Collingridge, R.W. Olsen, J. Peters, M. Spedding, Neuropharmacology 56 (2009) 2–5.
[29] R. Chittajallu, M. Vignes, K.K. Dev, J.M. Barnes, G.L. Collingridge, J.M. Henley, Nature 379 (1996) 78–81.
[30] J. Lerma, Nat. Rev. Neurosci. 4 (2003) 481–495.
[31] D.E. Jane, D. Lodge, G.L. Collingridge, Neuropharmacology 56 (2009) 90–113.
[32] J. Lerma, Nat. Neurosci. 14 (2011) 808–810.
[33] H. Herb, N. Burnashev, P. Werner, B. Sakman, W. Wisden, P.H. Seeburg, Neuron 8 (1992) 775–785.
[34] P. Werner, M. Voight, K. Keinänem, W. Wisden, P.H. Seeburg, Nature 351 (1991) 742–744.
[35] B. Bettler, J. Egebjerg, G. Sharma, G. Pecht, I. Hermans-Borgmeyer, C. Moll, C.F. Stevens, S. Heinemann, Neuron 8 (1992) 257–265.
[36] B. Sommer, N. Burnashev, T.A. Verdoon, K. Keinanem, B. Sakmann, P.H. Seeburg, EMBO J. 11 (1992) 1651–1656.
[37] T.H. Johansen, J. Drejer, F. Wätjen, E.Ø. Nielsen, Eur. J. Pharmacol. 246 (1993) 195–204.
[38] G.L. Collingridge, S.J. Kehl, H. McLennan, J. Physiol. 334 (1983) 33–46.
[39] H. Kamiya, S. Ozawa, J. Physiol. 509 (1998) 833–845.
[40] V.R. Clarke, G.L. Collingridge, Neuropharmacology 42 (2002) 889–902.
[41] V.R. Clarke, G.L. Collingridge, Neuropharmacology 47 (2004) 363–372.
[42] S.L. Dargan, V.R. Clarke, G.M. Alushin, J.L. Sherwood, R. Nisticò, Z.A. Bortolotto, A.M. Ogden, D. Bleakman, A.J. Doherty, D. Lodge, M.L. Mayer, S.M. Fitzjohn, D.E. Jane, G.L. Collingridge, Neuropharmacology 56 (2009) 121–130.
[43] J.F. Blake, M.W. Brown, G.L. Collingridge, Br. J. Pharmacol. 95 (1988) 291–299.
[44] A.M. Pugliese, E. Coppi, G. Spalluto, R. Corradetti, F. Pedata, Br. J. Pharmacol. 147 (2006) 524–532.
[45] A.M. Pugliese, E. Coppi, R. Volpini, G. Cristalli, R. Corradetti, L.S. Jeong, K.A. Jacobson, F. Pedata, Biochem. Pharmacol. 74 (2007) 768–779.
[46] C. Traini, F. Pedata, S. Cipriani, T. Mello, A. Galli, M.G. Giovannini, F. Cerbai, R. Volpini, G. Cristalli, A.M. Pugliese, Eur. J. Neurosci. 33 (2011) 2203–2215.
[47] V. Colotta, D. Catarzi, F. Varano, O. Lenzi, G. Filacchioni, C. Martini, L. Trincavelli, O. Ciampi, C. Traini, A.M. Pugliese, F. Pedata, E. Morizzo, S. Moro, Bioorg. Med. Chem. 16 (2008) 6086–6102.
[48] V. Colotta, O. Lenzi, D. Catarzi, F. Varano, G. Filacchioni, C. Martini, L. Trincavelli, O. Ciampi, A.M. Pugliese, C. Traini, F. Pedata, E. Morizzo, S. Moro, J. Med. Chem. 52 (2009) 2407–2419.
[49] S. Yamamoto, E. Tanaka, Y. Shoji, Y. Kudo, H. Inokuchi, H. Higashi, J. Neurophysiol. 78 (1997) 903–911.
[50] D.S. Pei, Q.H. Guan, Y.F. Sun, Q.X. Zhang, T.L. Xu, G.Y. Zhang, J. Neurosci. Res. 82 (2005) 642–649.
[51] D.S. Pei, X.T. Wang, Y. Liu, Y.F. Sun, Q.H. Guan, W. Wang, J.Z. Yan, Y.Y. Zong, T.L. Xu, G.Y. Zhang, Brain 129 (2006) 465–479.
[52] A.M. Buchan, H. Li, S. Cho, W.A. Pulsinelli, Neurosci. Lett. 132 (1991) 255–258.
[53] E. Le Peillet, B. Arvin, C. Moncada, B.S. Meldrum, Brain Res. 571 (1992) 115–120.
[54] B. Nellgard, T. Wieloch, J. Cereb. Blood Flow Metab. 12 (1992) 2–11.
[55] H. Furukawa, E. Gouaux, EMBO J. 22 (2003) 2873–2885.
[56] MOE (Molecular Operating Environment), version 2008.10; software available from Chemical Computing Group Inc. (1010 Sherbrooke Street West, Suite 910, Montreal, Quebec, Canada H3A 2R7); http://www.chemcomp.com.
[57] M. Wojciechowski, B. Lesyng, J. Phys. Chem. B 108 (2004) 18368–18376.
[58] W.D.C. Cornell, C.I. Bayly, I. Gould, K.M. Merz, D.M. Ferguson, D.C. Spellmeyer, T. Fox, J.W. Caldwell, P.A. Kollman, J. Am. Chem. Soc. 117 (1995) 5179–5196.
[59] C.A. Baxter, C.W. Murray, D.E. Clark, D.R. Westhead, M.D. Eldridge, Proteins Struct. Funct. Genet. 33 (1998) 367–382.
[60] T. Halgren, J. Comput. Chem. 17 (1996) 490–519.
[61] J.J.P. Stewart, MOPAC 7, Fujitsu Limited, Tokyo, Japan, 1993.
[62] E.O. Nielsen, U. Madsen, K. Schaumburg, L. Brehm, P. Krogsgaard-Larsen, Eur. J. Chem. Chim. Ther. 21 (1986) 433–437.
[63] G. Mannaioni, V. Carlà, F. Moroni, Br. J. Pharmacol. 118 (1996) 1530–1536.
[64] A. De Lean, P.J. Munson, D. Rodbared, Am. J. Physiol. 235 (1978) E97–102.
[65] Y.C. Cheng, W.H. Prusoff, Biochem. Pharmacol. 22 (1973) 3099–3108.
[66] W.W. Anderson, G.L. Collingridge, J. Neurosci. Methods 108 (2001) 71–83.
[67] F. Pedata, S. Latini, A.M. Pugliese, G. Pepeu, J. Neurochem. 61 (1993) 284–289.